X-ray-induced persistent photoconductivity in vanadium dioxide

S. H. Dietze, M. J. Marsh, Siming Wang, J.-G. Ramírez, Z.-H. Cai, J. R. Mohanty, Ivan K. Schuller, and O. G. Shpyrko

Phys. Rev. B **90**, 165109 — Published 8 October 2014

DOI: 10.1103/PhysRevB.90.165109

X-ray induced persistent photoconductivity in vanadium dioxide

S. H. Dietze,[1] M. J. Marsh,[1] Siming Wang,[1,2] J.-G. Ramírez,[1]
Z.-H. Cai,[3] J. R. Mohanty,[1] Ivan K. Schuller,[1] and O. G. Shpyrko[1,*]

[1] *Department of Physics and Center for Advanced Nanoscience, University of California, San Diego, La Jolla, CA 92093, USA*
[2] *Materials Science and Engineering Program, University of California, San Diego, La Jolla, CA 92093, USA*
[3] *Advanced Photon Source, Argonne National Laboratory, Argonne, IL 60439 ,USA*

(Dated: September 15, 2014)

The resistivity of vanadium dioxide (VO_2) decreased by over one-order of magnitude upon localized illumination with x-rays at room temperature. Despite this reduction, the structure remained in the monoclinic phase and had no signature of the high-temperature tetragonal phase that is usually associated with the lower resistance. Once illumination ceased, relaxation to the insulating state took tens of hours near room temperature. However, a full recovery of the insulating state was achieved within minutes by thermal cycling. We show that this behavior is consistent with random local-potential fluctuations and random distribution of discrete recombination sites used to model residual photoconductivity.

PACS numbers: 73.23.Ra, 73.50.Pz, 73.50.-h, 71.30.+h
Keywords: PPC, metal-insulator, vanadium oxide

INTRODUCTION

Metal oxides exhibit diverse ground states and phenomena including high-temperature superconductivity [1], colossal magnetoresistance [2], charge density waves [3], Verwey transitions [4], and metal-insulator transitions (MIT) [5]. Significant attention has been given to the deceptively simple MIT, which has to date been driven with temperature, electric field [6], pressure [7], chemical doping [8], ultrafast laser excitation [9], and ionizing radiation [10]. The MIT in VO_2 occurs above room temperature (340 K) with a simultaneous structural phase transition (SPT), changing from a semiconductor with a monoclinic lattice to a metal with a tetragonal lattice [5, 11, 12]. There is a variation of MIT temperatures between VO_2 grains, even for high quality samples [13]. Thus, metallic inclusions exist well below the bulk MIT temperature. The band bending at these metal-insulator interfaces can extend the lifetime of photogenerated electron-hole pairs, which contribute to conductivity [14].

Persistent photoconductivity (PPC) has been intensely studied in semiconductors [15, 16], superconductors [17], and metal oxides [10]. PPC is an increase in carrier concentration or mobility that is induced by electromagnetic radiation and remains for an extended period of time after illumination has ceased [18]. A long-lived photoinduced conversion to the metallic phase was previously observed in tungsten doped vanadium dioxide, but only below 50 K [19]. Additionally, a short-lived photoconductivity, decaying within tens of seconds, has been observed in vanadium oxide nano-devices [20–22]. However, long-lived photoconductivity has not been induced in pure VO_2 at room temperature until now. In addition, it was unclear if photoconductivity in VO_2 is coupled with the MIT and SPT. To better understand the driving mechanism of PPC in VO_2, we explored the relationship between crystal structure and PPC using localized x-ray radiation at room temperature. In this article, we show that photoillumination produced a large increase in conductance lasting for hours after illumination had ceased. Furthermore, we demonstrate that this dramatic change in conductance did not modify the metal-insulator transition temperature or change the crystal structure at the current resolution. Finally, to explain this effect we discuss and refute several possibilities, suggesting two well established models as candidates for PPC in VO_2.

SETUP AND SAMPLE

The vanadium dioxide (VO_2) thin film was prepared on an r-plane sapphire substrate by reactive RF magnetron sputtering. The target used in the deposition was a V_2O_3 pressed and sintered powder ceramic (1.5" diameter, >99.7%, ACI Alloys, Inc.). The sample was prepared in a high vacuum deposition system with a base pressure of 10^{-7} torr. A mixture of ultra high purity Ar and O_2 gases were used for sputtering. The total pressure during deposition was 4.0 mtorr, and the oxygen partial pressure was optimized to 3.4×10^{-4} torr (8.5% of the total pressure). The substrate temperature was 600 °C and the RF magnetron power was 100 W. The film reported here is 80 nm and was deposited at a rate of 0.17 Å/s. Due to the substrate interaction, the thin film grows polycrystalline, with grains randomly oriented in-plane, but with the (100) monoclinic direction out-of-plane.

The sample was cooled at a rate of 13°C/min in the same Ar/O_2 background gas of the deposition. On top of the VO_2 film, rectangular metallic electrodes were

deposited with 10 µm separation and 7 µm width using electron-beam lithography. A set of leads, for electrical connections, were patterned on top of the small electrodes using photolithography. The leads and electrodes were made by sputtering 50 nm vanadium, which acts as an adhesion layer, and 100 nm of gold to assure that the electrode resistance is lower than that of the metallic VO_2.

This sample exhibited three-orders magnitude resistance change when going through the metal-insulator transition (MIT), reaching a high-temperature resistance of approximately 25 Ω. Below 325 K, the resistance followed Mott insulating behaviour with an activation energy of (330 ± 10) meV. With an expected band gap of 600 meV [23], this is a good indication that our sample was only weakly doped with impurities.

The sample was mounted on a stage with a heater able to reach 400 K and a Pt100 RTD to measure temperature immediately adjacent to the sample. The stage is mounted to a Newport 6-circle Kappa diffractometer. A Princeton Quad-RO CCD is used to measure the (200) x-ray diffraction peak in the low-temperature monoclinic phase and the (101) peak in the high-temperature tetragonal phase. Both of these reflections are near the substrate normal direction and thus accessible for all grains in the film. A Vortex-EX x-ray fluorescence detector is used to locate the VO_2 device regions between the gold contacts. These gold contacts are used to measure resistance across the device by applying a voltage (V) referenced to ground and measuring the current (I). To ensure that no significant distortion of the electronic density of states occurred, we applied a small 50 V/cm electric field for our measurements [24]. We approximate the device resistance as V/I from this two-terminal measurement.

Primary measurements were performed at Sector 2-ID-D insertion device (micro-diffraction) beamline of the Advanced Photon Source. X-rays were produced via an undulator tuned to 10.3 keV and monochromatized by a Si (111) double-Bragg crystal. A pinhole was used in series with a zone plate to select only the first order focus. The focusing and incident angle gives a 250 nm × 950 nm x-ray footprint on the sample that determines the horizontal and vertical spatial resolution, respectively. The total photon flux is approximately 10^9 photons/second. All measurements were made in air at atmospheric pressure.

RESULTS

We probed a VO_2 device at room temperature (300 K) using focused x-rays. The illumination induced a photoconductance, which we define here as the measured conductance minus the conductance before x-ray illumination. The observed increases in photoconductance correlate with x-ray illumination of the device (Figure 1).

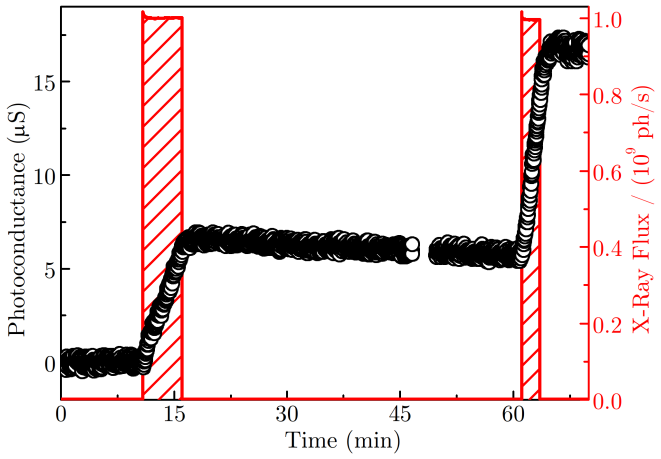

FIG. 1. (Color online). Photoconductance (black circles) of the VO_2 device at 300 K, showing rapid increase during x-ray illumination (dashed red region) as well as slow decrease after the x-ray illumination was turned off.

After the x-ray illumination ceased, the photoconductance gradually decreased and returned to zero within a week at room temperature. In addition, the x-ray exposure did not alter the MIT temperature. Heating the device through the MIT showed a sharp drop in resistance at the same temperature as before x-ray illumination (Fig. 2 (a)). This is in contrast to high-T_c cuprates, where illumination induces photoconductivity in the semiconducting state and modifies the superconducting transition temperature [16].

In a separate experiment, we illuminated the same device with a 650 nm (1.9 eV) laser focused to 100 µm × 100 µm. We estimate the device region was irradiated with 10^{14} ph/s or 30 µW power, which is over three orders of magnitude more power compared to the total x-ray power absorbed into the VO_2 film. The laser did not elicit a conductance change, indicating that any deep level impurities within the 0.6 eV band gap are not the cause for PPC in VO_2 [23]. This is in contrast with usual photoconductance in semiconductors, where a donor-complex model is often used [15].

A change in conductance due to the MIT is directly associated with the SPT and results in a change of the lattice parameters, which shows up as a shift in the location of the Bragg diffraction peaks. We have mapped the structural phase of the device, define by the gold contact pads (Fig. 2(b)), with and without photoconductance (Fig. 2(1c) to (3c)). We present these maps as the difference in the location of the measured Bragg peak and the mean Bragg peak of the low-temperature monoclinic phase, $\Delta Q = Q - \langle Q \rangle_M$. These maps show local variation due to strain of individual grains, common of thin films. At 300 K and 40 kΩ resistance, before significant x-ray exposure (Fig. 2(1c)), the out-of-plane Bragg peak was found in the monoclinic phase with $\langle Q \rangle_M =$

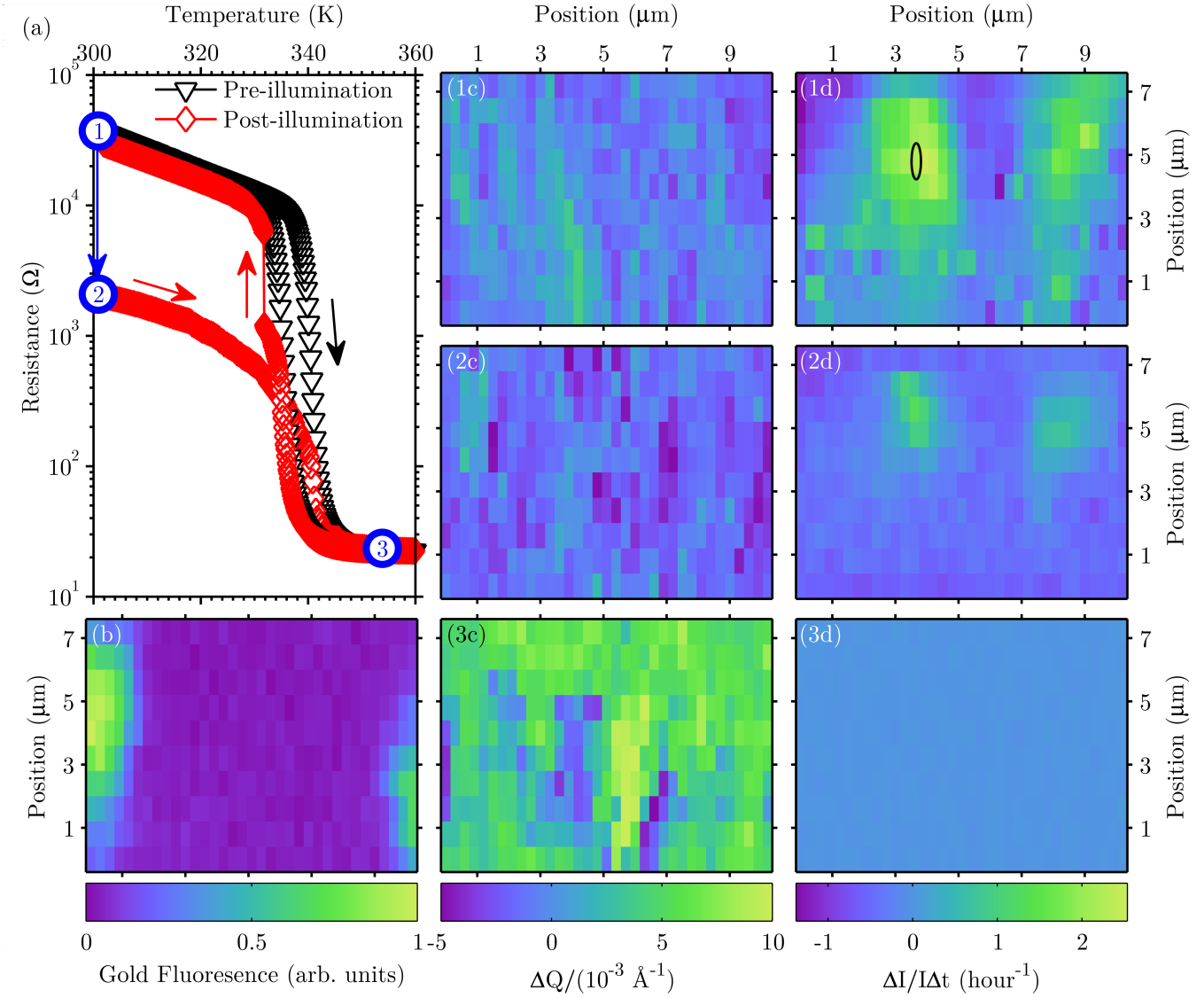

FIG. 2. (Color online). (a) The resistance is reduced by over one-order of magnitude at room temperature (point 1 to 2) by illuminating the device with x-rays at the indicated location in (1d) by the black ellipse. The resistance versus temperature hysteresis shows that the thermal component of the insulator-metal transition occurs at the same temperature for post-illumination (red diamonds) as no x-ray exposure (black down-pointing triangles). The original state is recovered by annealing the sample at 400 K and returning to room temperature. The device maps (b) to (d) are generated by scanning x-rays starting from the bottom-left corner proceeding in a series of horizontal lines. (b) Gold fluorescence intensity indicates the electrodes that define the device area. (c) Change in out-of-plane Bragg peak as compared to monoclinic phase and (d) normalized change in conductance induced by x-ray exposure for (1) 300 K and 40 kΩ resistance before significant x-ray exposure in the monoclinic phase with $\langle Q\rangle_M = 2.590\,\text{Å}^{-1}$ and $\langle \Delta I/I\Delta t\rangle_M = +0.3\,\text{h}^{-1}$; (2) 300 K and 2 kΩ resistance after x-ray exposure with $\langle Q\rangle_{PPC} = 2.589\,\text{Å}^{-1}$ and $\langle \Delta I/I\Delta t\rangle_{PPC} = -0.3\,\text{h}^{-1}$; (3) 354 K and 25 Ω resistance in the tetragonal phase with $\langle Q\rangle_R = 2.594\,\text{Å}^{-1}$ and $\langle \Delta I/I\Delta t\rangle_R = 0.0\,\text{h}^{-1}$.

$2.590\,\text{Å}^{-1}$. For comparison, at 354 K and 25 Ω resistance (Fig. 2(3c)), the out-of-plane Bragg peak was found at $\langle Q\rangle_R = 2.594\,\text{Å}^{-1}$. This is the expected $4\times10^{-3}\,\text{Å}^{-1}$ shift between the monoclinic phase at 300 K and the tetragonal phase at 354 K [25]. Near the MIT, a coexistence of the high- and low-temperature phases is known to occur [13, 26, 27]. After approximately 45 minutes of x-ray exposure at the location indicated by the black ellipse in Fig. 2(1d), the room temperature resistance dropped from 40 kΩ to 2 kΩ (point 1 to 2 on Fig. 2(a)). However, the sample was not modified toward the high-temperature (tetragonal) structure, having a mean out-of-plane Bragg peak of $\langle Q\rangle_{PPC} = 2.589\,\text{Å}^{-1}$.

Although, a change in conductance can be induced by x-ray illumination of a single location and did not require any scanning of the device, the photoresponse varied

across the device (Fig. 2(1d) to (3d)). By photoresponse we mean a change in conductance during a short eight second period of localized illumination. We scanned the device using continuous illumination. Thus, it is possible to observe a negative photoresponse due to relaxation of photoconductance induced at previously scanned locations. The relaxation is approximately $-1.3\,\mathrm{h}^{-1}$, shown in Fig. 1, during no illumination, matching well to the minimum observed of $-1.4\,\mathrm{h}^{-1}$ for some regions, suggesting there is no actual negative photoresponse but only decay of previously generated photoconductance. Initially, the photoresponse was very strong in two large regions of the device, with a maximum of $+2.5\,\mathrm{h}^{-1}$ and mean of $+0.3\,\mathrm{h}^{-1}$ (Fig. 2 (1d)). Although these variations in photoresponse to some extent agree with the variations in high-temperature structural phase, the correlation is weak. There is no statistically significant difference in the crystal structure for regions exhibiting strong and weak photoresponse. After significant illumination, the strong photoresponse regions shrank in size, now with maximum of $+1.3\,\mathrm{h}^{-1}$ (Fig. 2 (2d)). Most of the region can no longer sustain the immediate photoconductance giving a mean photoresponse of $-0.3\,\mathrm{h}^{-1}$. For comparison, at 354 K in the metallic state (25 Ω), the conductance is stable and no photoresponse is observed (Fig. 2 (3d)).

At 330 K, just below the MIT temperature, we observed a slow decay of photoconductance after x-ray illumination is stopped (Fig. 3). Given that the photoconductance decays continuously to zero, an accurate fit was made by using a stretched exponential of the form,

$$G_0 \exp\left[-(t/\tau)^{\beta}\right]. \quad (1)$$

This function is commonly used to describe relaxation toward equilibrium in a wide variety of systems including those exhibiting PPC due to random local-potential fluctuations [18, 28] and discrete random traps [29]. The stretched exponential fit agrees with the observed photoconductance decay over the entire range. We extract a time constant of $\tau = (54 \pm 1)$ h and a stretching exponent of $\beta = 0.69 \pm 0.01$. This gives a mean relaxation time of (69 ± 1) h.

The PPC relaxation time was significantly reduced by thermal cycling the VO_2 well above the MIT temperature. After annealing the device at 400 K for 20 minutes without illumination, it recovered the original resistance upon cooling (red diamond curve of Fig. 2(a)).

DISCUSSION

The persistent nature of the photoconductance is not consistent with a thermally induced MIT. The x-ray power used was 1.6 µW, only 1.5% of which is absorbed into the 80 nm thick sample, calculated from the attenuation coefficient and the illumination angle. The Al_2O_3 substrate has a much smaller attenuation coefficient and

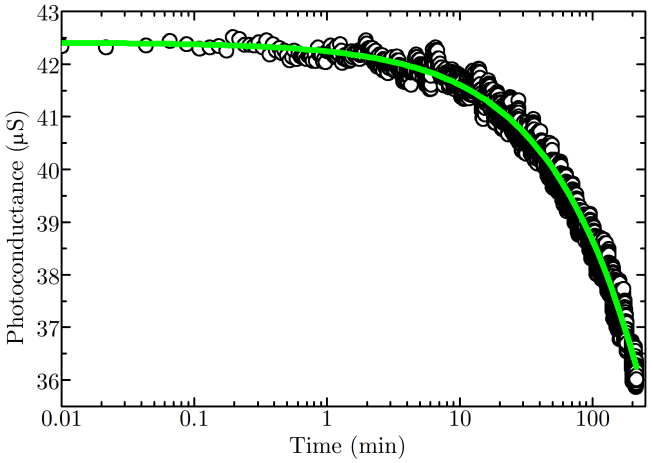

FIG. 3. (Color online). Decay of photoconductance at 330 K post-illumination. The green line is a fit using a stretched exponential with the additional information that the photoconductance eventually returns to zero. The mean relaxation time is 69 hours.

a much larger thermal conductivity compared to VO_2 and thus acts as a thermal sink. From the heat transport equation and known thermal properties of VO_2 at room temperature, we calculate that at equilibrium the x-ray heat loading of the entire device was less than 0.1 mK. This does not account for further losses due to atmosphere, which would further reduce this number. Since, the sample temperature is stabilized approximately 35 K below the MIT temperature, the x-ray power is insufficient to raise the temperature of the device to cause a significant change in the measured resistance. Since the x-ray beam was highly focused, a thermoelectric current could result from localized heating near the gold contacts that are used for electrical transport measurements. However, a positive thermoelectric current due to heating near one contact would mean a negative thermoelectric current at the opposite contact [30]. We did not see this asymmetric response during localized illumination across the device (Fig. 2 (1d) and (2d)).

A previous observation of x-ray induced conductance increase in tungsten doped VO_2 was due to the formation of metallic puddles that exhibit the high-temperature (tetragonal) crystal structure [19]. It is suggested that each ionizing photon causes the dissociation of many V-V dimers, effectively converting the insulating phase to metal. A conversion to the metallic phase via the above process is expected to nucleate near the illuminated volume and spread isotropically, possibly in a random-resistor network fashion due to variations in the sample. To account for the one-order magnitude decrease in resistance that we have observed, our VO_2 device would need to be at least 37% volume metal fraction. Since we have observed no appreciable shift in the Bragg diffraction peak towards the tetragonal structure post-illumination

(Fig. 2 (2c)), the generation of metallic puddles cannot be the cause for PPC in our VO_2 device.

It is noteworthy, that a metallic surface or filaments could also lead to the observed increase in conductance. In this case, the metal fraction would be a minimum of 1.2% of the device volume, if they extend uniformly from one electrode to the other. The diffraction signal would then mostly be indistinguishable from the insulating phase. However, a metallic surface created by a change in vanadium oxidation state, similar to PPC in ZnO [31, 32], is not likely. To observe an increase in conductance, VO_2 would need to be reduced [33]. Since the beam is well localized, yet a large portion of the surface must participate to account for the photoconductance, a significant oxygen mobility would be required, which is only seen for layered or amorphous materials [34]. Therefore, if the observed PPC is associated with a structural transition, it must come in the form of a large number of narrow metallic filaments, since a single filament of the minimum required 85 nm width would still be detected. For instance, it is possible that a change in conductance is primarily confined to grain boundaries or other extended defects, however at the current resolution this cannot be determined.

An estimated total of 10^{10} photons were absorbed into the VO_2 film when we observed a one-order magnitude decrease in resistance at room temperature (300 K). If one photocarrier is generated per photon, such carriers would need a mobility of $0.1\,\mathrm{cm}^2/(\mathrm{V\,s})$ to account for the resistance change. This is within the known range of electron mobility in the insulating phase for VO_2 of $(0.1 \text{ to } 1)\,\mathrm{cm}^2/(\mathrm{V\,s})$ [35]. This indicates that an increase in carrier concentration is the cause for the change in conductance.

The long recombination time of photoinduced carriers is generally explained by phonon-assisted hopping or tunneling of potential barriers [36]. Using the simple Arrhenius model, the time for hopping of a potential barrier is given by,

$$t = t_0 \exp\left(\tfrac{E}{k_B T}\right), \tag{2}$$

where t_0 is the inverse of the electron-hole recombination attempt rate, E is the activation energy (potential barrier), k_B is the Boltzmann constant and T is the temperature of the system. Since, systems exhibiting local-potential fluctuations do not strictly follow the expected temperature dependent decay time [20], we shall estimate the potential barrier by using the standard attempt rate of 1 THz induced by phonons [37]. We thus calculate the average effective activation energy as (1.1 ± 0.2) eV, where the error is given by using a three order magnitude deviation of the attempt rate (i.e. 1 GHz to 1 PHz). This is almost twice as large as the 0.6 eV VO_2 band gap [23]. Other oxides, such as ZnO, also show an activation energy of roughly 1 eV [31]. This is in contrast to the donor-complex model used for semiconductors, as the barrier is always less than the band gap. For example, both $Al_{0.3}Ga_{0.7}As$ and $Zn_{0.3}Cd_{0.7}Se$ have approximately 0.1 eV barriers with a direct band gap of 1.9 eV and 2.0 eV, respectively [15, 28, 38–41]. The large energy barrier observed could be due to a number of things including VO_x phase boundaries, where the conduction bands can change significantly or due to a much smaller variation in $VO_{2+\delta}$, but requiring a collective electron/hole hopping.

A number of models have been developed to describe persistent photoconductivity in various materials. It is known that even high quality VO_2 thin films exhibit inhomogeneities, such as nonstoichiometry and grain boundaries, which are responsible for the microscopic phase coexistence far below the bulk MIT temperature [13, 26, 27]. Photogenerated electron-hole pairs can be separated due to band bending at these metal-insulator phase boundaries. The long recombination time is likely the result of random local-potential fluctuations and/or a random distribution of discrete recombination sites, due to these inhomogeneities [28, 29]. With discrete sites, the relaxation becomes stretched [42]. However, our observed value of $\beta = 0.69$ is slightly larger than the expected value of $\frac{3}{5}$ for 3-dimensional systems [43]. This increase is often observed near and above the MIT temperature where electron correlations are reduced and simple (Debye) exponential relaxation is recovered [44].

CONCLUSION

Although we have reported on only one VO_2 device, we have carefully measured and consistently found residual photoconduction in five samples, prepared by various growers from different laboratories. Focused x-ray radiation reversibly altered the device conductance without modifying the MIT transition temperature or high-temperature resistance. In addition, the structural transition was not induced for any sizable convex region as compared to the imaging resolution. Two distinct geometric possibilities exist to explain this. In the first case, a relatively weak additional conductance channel is created over a large portion of the device. This channel would be completely decoupled from the MIT and SPT. In the second case, illumination causes a stable transition to the metallic state along narrow filaments, likely along grain boundaries. These two cases could be distinguished by using local conductance measurements.

The mechanism for long-term stability of photoconductivity is still open for discussion. To further the understanding of PPC in VO_2, it should be confirmed that the photoconductivity is indeed an increase in carrier concentration. This could be done by obtaining the mobility of carriers from Hall measurements pre- and post-illumination [45].

ACKNOWLEDGMENTS

This work was supported by AFOSR FA9550-12-1-0381. Use of the Advanced Photon Source, an Office of Science User Facility operated for the U.S. Department of Energy (DOE) Office of Science by Argonne National Laboratory, was supported by the U.S. DOE under Contract No. DE-AC02-06CH11357. X-ray microscopy measurements are supported by U.S. Department of Energy, Office of Science, Office of Basic Energy Sciences, under Contract DE-SC0001805.

* Author to whom any correspondence should be addressed. oshpyrko@physics.ucsd.edu

[1] M. K. Wu, J. R. Ashburn, C. J. Torng, P. H. Hor, R. L. Meng, L. Gao, Z. J. Huang, Y. Q. Wang, and C. W. Chu, Phys. Rev. Lett. **58**, 908 (1987).

[2] A. J. Millis, Nature **392**, 147 (1998).

[3] S. Cox, J. Singleton, R. D. McDonald, A. Migliori, and P. B. Littlewood, Nature **7**, 25 (2008).

[4] J. P. Attfield, A. M. T. Bell, L. M. Rodriguez-Martinez, J. M. Greneche, R. J. Cernik, J. F. Clarke, and D. A. Perkins, Nature **396**, 655 (1998).

[5] F. J. Morin, Phys. Rev. Lett. **3**, 34 (1959).

[6] H.-T. Kim, B.-G. Chae, D.-H. Youn, G. Kim, K.-Y. Kang, S.-J. Lee, K. Kim, and Y.-S. Lim, Appl. Phys. Lett. **86**, 242101 (2005).

[7] E. Arcangeletti, L. Baldassarre, D. Di Castro, S. Lupi, L. Malavasi, C. Marini, A. Perucchi, and P. Postorino, Phys. Rev. Lett. **98**, 196406 (2007).

[8] W. Burkhardt, T. Christmann, S. Franke, W. Kriegseis, D. Meister, B. Meyer, W. Niessner, D. Schalch, and A. Scharmann, Thin Solid Films **402**, 226 (2002).

[9] A. Cavalleri, C. Tóth, C. W. Siders, J. A. Squier, F. Ráksi, P. Forget, and J. C. Kieffer, Phys. Rev. Lett. **87**, 237401 (2001).

[10] V. Kiryukhin, D. Casa, J. P. Hill, B. Keimer, A. Vigliante, Y. Tomioka, and Y. Tokura, Nature **386**, 813 (1997).

[11] J. B. Goodenough, J. Solid State Chem. **3**, 490 (1971).

[12] A. Zylbersztejn and N. F. Mott, Phys. Rev. B **11**, 4383 (1975).

[13] J.-G. Ramírez, A. Sharoni, Y. Dubi, M. E. Gómez, and I. K. Schuller, Phys. Rev. B **79**, 235110 (2009).

[14] C. Miller, M. Triplett, J. Lammatao, J. Suh, D. Fu, J. Wu, and D. Yu, Phys. Rev. B **85**, 085111 (2012).

[15] D. V. Lang, R. A. Logan, and M. Jaros, Phys. Rev. B **19**, 1015 (1979).

[16] G. Nieva, E. Osquiguil, J. Guimpel, M. Maenhoudt, B. Wuyts, Y. Bruynseraede, M. B. Maple, and I. K. Schuller, Appl. Phys. Lett. **60**, 2159 (1992).

[17] A. Hoffmann, J. Hasen, D. Lederman, T. Endo, Y. Bruynseraede, and I. K. Schuller, J. Alloys Compd. **251**, 87 (1997).

[18] M. K. Sheinkman and A. Y. Shik, Sov. Phys. Semicond. **10**, 128 (1976), [Fiz. Tekh. Poluprovodn. **10**, 209 (1976)].

[19] K. Shibuya, D. Okuyama, R. Kumai, Y. Yamasaki, H. Nakao, Y. Murakami, Y. Taguchi, T. Arima, M. Kawasaki, and Y. Tokura, Phys. Rev. B **84**, 165108 (2011).

[20] J. Park, E. Lee, K. W. Lee, and C. E. Lee, Appl. Phys. Lett. **89**, 183114 (2006).

[21] H. Kweon, K. W. Lee, and C. E. Lee, Appl. Phys. Lett. **93**, 043105 (2008).

[22] K. W. Lee, H. Kweon, J. Park, and C. E. Lee, Appl. Phys. Lett. **94**, 233111 (2009).

[23] H. W. Verleur, A. S. Barker, and C. N. Berglund, Rev. Mod. Phys. **40**, 737 (1968).

[24] P. Boriskov, A. Velichko, A. Pergament, G. Stefanovich, and D. Stefanovich, Tech. Phys. Lett. **28**, 406 (2002).

[25] K. D. Rogers, Powder Diffr. **8**, 240 (1993).

[26] M. M. Qazilbash, M. Brehm, B.-G. Chae, P.-C. Ho, G. O. Andreev, B.-J. Kim, S. J. Yun, A. V. Balatsky, M. B. Maple, F. Keilmann, H.-T. Kim, and D. N. Basov, Science **318**, 1750 (2007).

[27] M. M. Qazilbash, A. Tripathi, A. A. Schafgans, B.-J. Kim, H.-T. Kim, Z. Cai, M. V. Holt, J. M. Maser, F. Keilmann, O. G. Shpyrko, and D. N. Basov, Phys. Rev. B **83**, 165108 (2011).

[28] H. X. Jiang and J. Y. Lin, Phys. Rev. Lett. **64**, 2547 (1990).

[29] D. L. Huber, Phys. Rev. B **31**, 6070 (1985).

[30] J. Cao, W. Fan, H. Zheng, and J. Wu, Nano Lett. **9**, 4001 (2009).

[31] S. A. Studenikin, N. Golego, and M. Cocivera, J. Appl. Phys. **87**, 2413 (2000).

[32] Q. H. Li, T. Gao, Y. G. Wang, and T. H. Wang, Appl. Phys. Lett. **86**, 123117 (2005).

[33] C. C. Kwan, C. Griffiths, and H. Eastwood, Appl. Phys. Lett. **20**, 93 (1972).

[34] V. I. Kudinov, I. L. Chaplygin, A. I. Kirilyuk, N. M. Kreines, R. Laiho, E. Lähderanta, and C. Ayache, Phys. Rev. B **47**, 9017 (1993).

[35] C. N. Berglund and H. J. Guggenheim, Phys. Rev. **185**, 1022 (1969).

[36] M. Ben-Chorin, Z. Ovadyahu, and M. Pollak, Phys. Rev. B **48**, 15025 (1993).

[37] F. Gervais and W. Kress, Phys. Rev. B **31**, 4809 (1985).

[38] D. V. Lang and R. A. Logan, Phys. Rev. Lett. **39**, 635 (1977).

[39] H. X. Jiang, G. Brown, and J. Y. Lin, J. Appl. Phys. **69**, 6701 (1991).

[40] M. El Allali, C. B. Sørensen, E. Veje, and P. Tidemand-Petersson, Phys. Rev. B **48**, 4398 (1993).

[41] J. Ye, T. Yoshida, Y. Nakamura, and O. Nittono, Appl. Phys. Lett. **67**, 3066 (1995).

[42] R. Friedberg and J. M. Luttinger, Phys. Rev. B **12**, 4460 (1975).

[43] J. C. Phillips, Phys. Rev. B **52**, R8637 (1995).

[44] G. Beadie, E. Sauvain, A. S. L. Gomes, and N. M. Lawandy, Phys. Rev. B **51**, 2180 (1995).

[45] M. C. Tarun, F. A. Selim, and M. D. McCluskey, Phys. Rev. Lett. **111**, 187403 (2013).